

# Role of work function distribution on field emission effects

Nandan Pakhira<sup>1</sup> and Rajib Mahato<sup>1,2</sup>

<sup>1</sup>*Department of Physics, Kazi Nazrul University, Asansol, West Bengal 713340, India*

<sup>2</sup>*Central Electronics Engineering Research Institute, Pilani, Rajasthan 333031, India*

Field emission effect is the emission of electrons from a cold metallic surface in the presence of an electric field. The emission current exponentially depends on the work function of the metallic surface. In this work we consider the role of work function distribution on the field emission current. The work function distribution can arise due to nano-scale inhomogeneities of the surface as well as for collection of nano-particles with size distribution. We consider both Gaussian distribution as well as log-normal distribution. For Gaussian distribution, the field emission current,  $J_{av}$ , averaged over work function distribution shows Gaussian dependence,  $J_{av} \propto \exp(\alpha\sigma^2)$ , where  $\sigma$  is the width of the work function distribution and  $\alpha$  is a fitting parameter. For log-normal distribution,  $J_{av}$  shows compressed exponential behaviour,  $J_{av} \propto \exp(\gamma\sigma^n)$ , where the exponent  $n > 1$  is a non-universal parameter. We also study in detail field emission current for various electric field strength applied to systems with high density, characterised by Fermi energy,  $E_F \gg \Phi$ ,  $\Phi$  being the work function of the system as well as systems with low density characterised by  $E_F \ll \Phi$ .

## I. INTRODUCTION

Field emission is the process in which electrons from cold surfaces are emitted in the presence of applied strong electric field. This process should be compared against the thermo-ionic process in which electrons are emitted from hot metal surface. The field emission forms the backbone of modern semiconductor devices. This effect was first described by Fowler and Nordheim<sup>1</sup>. They considered quantum mechanical tunneling through a triangular potential energy (PE) barrier, created by the application of constant electric field. Much later Murphy and Good<sup>2</sup> (MG) introduced a more realistic PE barrier by taking into account the induced image charge formed in the presence of emitted electron. MG calculated barrier transmission coefficient under semi-classical WKB approximation. More recently, essentially an exact solution of the problem was obtained by Choy et. al.<sup>3</sup>. Also, various cases including finite temperature (thermal emission), tunneling, curvature of the emission surface have been considered by various authors<sup>4-11</sup>

To the best of our knowledge in all of those studies authors have considered constant *local* work function. The work function of a material depends on the composition, structure, geometry, local charge distribution etc. of the emitting surface. Assumption of constant work function is only suitable for an atomistic smooth homogeneous surface. For surfaces with inhomogeneities over nano-scale (much smaller than the size of the collectors) assumption of constant work function is no longer valid. Also it has been shown<sup>12</sup> that in a system of nano-particles there is a distribution of the size of the nano-particles. Since the work function is more of a property of the surface we naturally can expect that the work function of nano-particles will also have a distribution. The actual microscopic model for work function distribution for a system of nano-particles is beyond the scope of this work. Interestingly, Gamez et. al.<sup>12</sup> using scanning tunneling microscope (STM) have measured the pair distribution function (PDF) for Pt nano-particles and they

found that it follows log-normal distribution.

In this work, purely as a mathematical model, we choose Gaussian and log-normal distribution for the work function. We then study the field emission current averaged over work function distribution. The organization of the rest of the paper is as follows. In Sec. II we describe the mathematical formalism used to calculate field emission current. In Sec. III we describe the work function distribution used to calculate average current. In Sec. IV we present our results for both the case of Gaussian distribution and log-normal distribution. Finally in Sec. V we conclude.

## II. MATHEMATICAL FORMALISM

We closely follow and summarize the results obtained by Lopes et. al.<sup>13,14</sup> for field-emission current density,  $J$ . In the standard FN-type MG theory the field emission current density is given by the well known expression<sup>15-18</sup>,

$$J = \frac{e^3 \mathcal{E}^2}{16\pi^2 \hbar \Phi} \frac{1}{t^2(y_0)} \exp\left(-\frac{4}{3} \frac{\sqrt{2m}}{\hbar} \frac{\Phi^{3/2}}{e\mathcal{E}} v(y_0)\right) \quad (1)$$

where  $e$  and  $m$  are the charge and mass of electron,  $\mathcal{E}$  is the strength of the applied electric field,  $\Phi$  is the local work function of the emitting surface and

$$v(y) = \left[\frac{1 + \sqrt{1 - y^2}}{2}\right]^{1/2} \left[E(\lambda) - \left(1 - \sqrt{1 - y^2}\right) K(\lambda)\right] \quad (2)$$

$K(\lambda)$  and  $E(\lambda)$  are the complete elliptic integral of the first and second kind, with

$$\lambda^2 = \frac{2\sqrt{1 - y^2}}{1 + \sqrt{1 - y^2}} \quad (3)$$

and

$$y^2 = \frac{e^3 \mathcal{E}}{4\pi\epsilon_0(V_0 - E)^2} < 1. \quad (4)$$

It is important to mention that  $V_0 = \Phi + E_F$  is the height of the potential energy barrier ( $E_F$  is the Fermi energy) and  $E$  is the energy of the electron. Finally,

$$t(y_0) = \left[ v(y) - \frac{2}{3} y \frac{dv}{dy} \right]_{y=y_0} \quad (5)$$

with

$$y_0^2 = \frac{e^3 \mathcal{E}}{4\pi\epsilon_0 \Phi^2} \quad (6)$$

From the relations above it is quite evident that calculation of transmission current requires evaluation of numerical integrals for complete elliptic integrals. Due to the singularities present in complete elliptic integrals it is very hard to extract meaningful results purely numerically<sup>19</sup>. Under this circumstances we can consider series expansion for complete elliptic integrals<sup>20</sup> as follows

$$E(q) = 1 + \frac{1}{2} \left[ \ln \left( \frac{4}{q} \right) - \frac{1}{2} \right] q^2 + \dots \quad (7)$$

$$K(q) = \ln \left( \frac{4}{q} \right) + \left[ \ln \left( \frac{4}{q} \right) - 1 \right] \frac{q}{4} + \dots \quad (8)$$

where

$$q = \sqrt{1-p^2} \quad (9)$$

and  $p^2 = \frac{x_2 - x_1}{x_2}$ .  $x_1$  and  $x_2$  are the roots of the quadratic equation

$$V_0 - E - \frac{Ze^2}{4x} - e\mathcal{E}x = 0 \quad (10)$$

As a detailed calculation gives the following form for the field emission current density

$$J = \frac{e^3 \mathcal{E}^2}{16\pi^2 \hbar \Phi} \frac{[1 - u(y_0)]}{t^2(y_0)} \exp \left[ -\frac{4}{3} \sqrt{\frac{2m}{\hbar^2}} \frac{\Phi^{3/2}}{e\mathcal{E}} v(y_0) \right] \quad (11)$$

where

$$u(y_0) = \left[ 1 + \frac{2\sqrt{2m\Phi} E_F}{e\hbar} \frac{E_F}{\mathcal{E}} t(y_0) \right] \exp \left[ -\frac{2\sqrt{2m\Phi} E_F}{e\hbar} \frac{E_F}{\mathcal{E}} t(y_0) \right] \quad (12)$$

with

$$v(y_0) = 1 - \left[ \frac{3}{8} Z' \ln \left( \frac{8}{\sqrt{Z'}} \right) + \frac{Z'}{16} \right] + \frac{3}{8} Z' y_0^2 \ln(y_0) + \frac{Z'^2}{32} \left[ 1 - \ln \left( \frac{8}{\sqrt{Z'}} \right) \right] y_0^4 + \frac{Z'^2}{32} y_0^4 \ln(y_0) + \dots \quad (13)$$

and

$$t(y_0) = v(y_0) - \frac{2}{3} y_0 \frac{dv}{dy}(y_0) \quad (14)$$

with  $y_0$  given by Eq. 6 and  $Z' = 1.179$  is an arbitrary constant obtained from suitable boundary condition<sup>13</sup>.

The expression for transmission current in Eq. 11 carries an interesting pre-exponential factor  $[1 - u(y_0)]$  as compared to the standard form in Eq. 1. This factor exhibits an explicit dependence on the external electric field ( $\mathcal{E}$ ), work function ( $\Phi$ ) and Fermi energy,  $E_F$ .

It is worth to mention that, from Eq. 11, we can immediately investigate two important particular cases depending on the value of  $E_F$ . For large values of Fermi energies, i.e.,  $\frac{2\sqrt{2m}\Phi^{1/2}E_F}{e\hbar} \gg 1$ , or equivalently  $E_F \gg \frac{e\hbar\mathcal{E}}{2\sqrt{2m\Phi}}$ , it is easy to see that  $u(y_0) \approx 0$  in Eq. 12 since the exponential dominates. So, in this limit we recover the standard FN-type MG equation.

On the other hand, for the opposite regime, i.e., for very small Fermi energies, we have  $E_F \ll \frac{e\hbar\mathcal{E}}{2\sqrt{2m\Phi}}$ . In this limit we can expand the exponential in Eq. 12 and get

$$J = \frac{me}{2\pi^2 \hbar^3} E_F^2 \exp \left( -\frac{4}{3} \sqrt{\frac{2m}{\hbar^2}} \frac{\Phi^{3/2}}{e\mathcal{E}} v(y_0) \right) \quad (15)$$

It is worth to emphasize that for small values of Fermi energies a very different expression, compared to the standard FN-type MG formula, was obtained<sup>13</sup> for the current density. Note that in this regime the pre-exponential factor in Eq. 15 does not depend on either  $t(y_0)$  or the external electric field ( $\mathcal{E}$ ), but it remains dependent on the Fermi energy ( $E_F$ ).

### III. WORK FUNCTION DISTRIBUTION

In the previous section we have summarized field emission current for a given *local* work function  $\Phi$ . For a system of nano-particles or systems with inhomogeneity the work function will be different over the length scale of the size of the collector for emitted electrons. In such a situation we need to average the field emission current over the distribution of work function as follows :

$$J_{av} = \int P(\Phi) J(\Phi, E_F) d\phi \quad (16)$$

where  $P(\Phi)$  is the distribution of the work function,  $\Phi$ . We choose *two* widely used distribution functions, namely (i) Gaussian and (ii) log-normal distribution. It is well known that systems with *bulk disorder* follows Gaussian distribution and the work function distribution function,  $P(\Phi)$ , is given by

$$P_N(\Phi) = \frac{1}{\sigma\sqrt{2\pi}} \exp \left[ -\frac{(\Phi - \Phi_0)^2}{2\sigma^2} \right], \quad (17)$$

where  $\sigma$  is the *standard deviation* of the distribution and  $\Phi_0$  is the known *bulk* value for a given material.

We also use log-normal distribution for the work function :

$$P_{LN}(\Phi) = \frac{1}{\Phi\sigma\sqrt{2\pi}} \exp \left[ -\frac{(\ln \Phi - \mu)^2}{2\sigma^2} \right] \quad (18)$$

It is important to mention that we were inspired by the experimental result of Gamez et. al.<sup>12</sup>. They showed that for a system of Pt nano-particles the pair distribution function (PDF) for the radius of nano-particles follows log-normal distribution

$$F(r) = \frac{1}{rs\sqrt{2\pi}} \exp\left[-\frac{(\ln r - \mu)^2}{2s^2}\right] \quad (19)$$

with

$$s^2 = \ln\left[\left(\frac{P_{\text{sig}}}{P_{\text{size}}}\right) + 1\right] \quad (20)$$

$$\mu = \ln(P_{\text{size}}) - \frac{s^2}{2} \quad (21)$$

where  $P_{\text{size}}$  and  $P_{\text{sig}}$  are the average particle diameter and standard deviation, respectively. Since work function crucially depends on the surface properties of a system it may follow log-normal distribution as in the case of *surface disorder*.

Various statistical properties of this distribution are summarized in the table I :

TABLE I: Statistical properties of log-normal distribution

Mean	$e^{\mu + \frac{\sigma^2}{2}}$
Variance	$\nu = e^{2\mu + 2\sigma^2} [e^{\sigma^2} - 1]$
Standard deviation	$s = \sqrt{\nu}$
Median	$M = e^{\mu}$
Mode	$\Gamma = e^{\mu - \sigma^2}$
Skewness	$\Sigma = (e^{\sigma^2} + 2)\sqrt{e^{\sigma^2} - 1}$
Kurtosis	$\kappa = e^{4\sigma^2} + 2e^{3\sigma^2} + 3e^{2\sigma^2} - 3$

## IV. RESULTS

In this section we show our results for current density averaged over two choice of probability distributions as have been discussed in the previous section.

### A. Gaussian work function distribution

We first consider the case of Gaussian distribution for the work function. In Fig. 1 we show the histogram plot of the work function, sampled over Gaussian distribution for *four* choices of *bulk* work function  $\Phi_0 = 3.0, 3.5, 4.0$  and  $4.5$  eV with  $\sigma = 0.05$ . In each case we also fit the histogram plot to Gaussian distribution. From this fit we can see that our choice of random variables for  $\Phi$  are well sampled over Gaussian distribution.

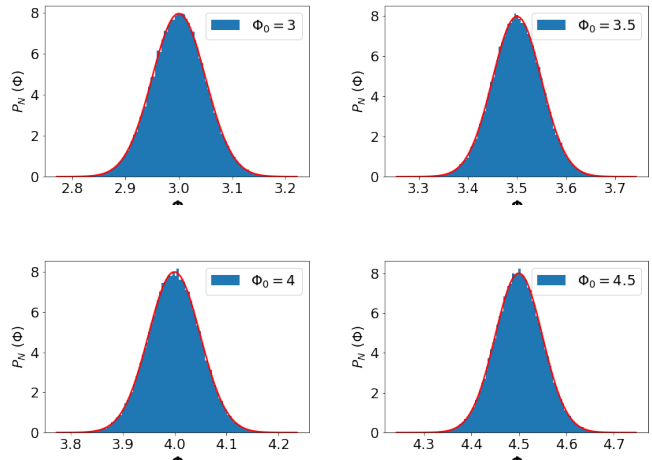


FIG. 1: (Color online) Histogram plot of work function,  $\Phi$ , sampled over Gaussian distribution for various average work function,  $\Phi_0$ . Solid line shows fitting to Gaussian distribution and we have chosen  $\sigma = 0.05$  for all the cases.

#### 1. Case with $\Phi \ll E_F$

We now consider the case with  $E_F = 10$  eV and  $\Phi_0 = 3.0, 3.5, 4.0$  and  $4.5$  eV. Since  $E_F \propto n^{2/3}$ ,  $n$  being the density of electrons, this will correspond to high density limit. In Fig. 2 we show the current density averaged over various number of random variables,  $N$ , for  $\Phi$ . For  $N < 10^4$  there is significant fluctuations of  $J_{\text{av}}$  but for  $N > 4 \times 10^4$ ,  $J_{\text{av}}$  show small fluctuations over mean value. We choose  $N = 10^5$  for calculation of  $J_{\text{av}}$  for all the cases and  $J_{\text{av}}$  will be free of *statistical errors*.

As shown in Fig. 2,  $J_{\text{av}}$  varies over several orders of magnitude as we vary  $\Phi_0$  from 3.0 eV to 4.5 eV. So in order to understand role of work function distribution on field emission current we need to study the dimensionless scaled quantity  $J_{\text{av}}/J_0$ , where  $J_0$  is the field emission current for *bulk* value of the work function  $\Phi_0$  and can be calculated from Eq. 1 with  $\Phi = \Phi_0$ .

In Fig. 3 we show,  $\log(J_{\text{av}}/J_0)$ , as a function of the width of the work function distribution,  $\sigma$  for a given applied electric field,  $\mathcal{E} = 3 \times 10^7$  V/cm. We choose  $0.01 \leq \sigma \leq 0.1$ . Since the full width at half maxima (FWHM) for a Gaussian distribution is  $2.35\sigma$  and more than 95% integrated weight is within a width  $4\sigma$  (between  $-2\sigma$  and  $+2\sigma$ ) our choice of  $\sigma$  ensures that the deviation of  $\Phi$  from its bulk value  $\Phi_0$  is less than 10%. The first noticeable feature in Fig. 3 is that the current density,  $J_{\text{av}}$ , averaged over work function distribution increases monotonically with the width of the distribution,  $\sigma$ . This is because the transport current,  $J(\Phi) \propto \exp(-\zeta\Phi^{3/2})$  where  $\zeta = \frac{4}{3}\sqrt{\frac{2m}{\hbar^2}}\frac{v(y_0)}{e\mathcal{E}}$  and the averaging over work function distribution leads to exploration of regions with lower

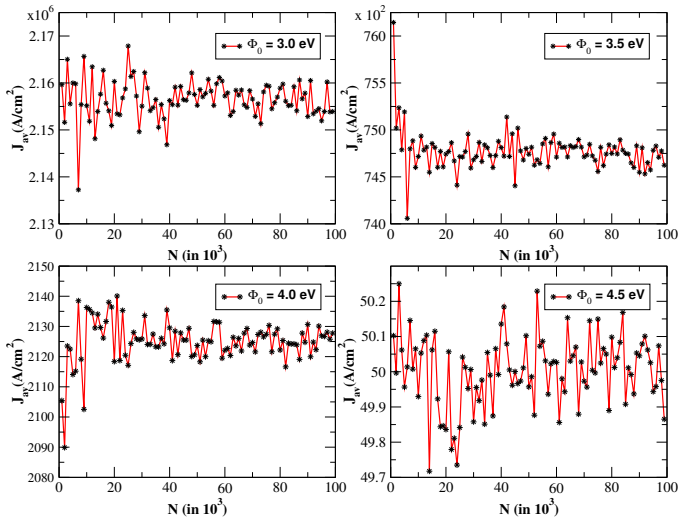


FIG. 2: (Color online) Average current,  $J_{av}$ , as a function of number of random variables,  $N$  chosen from Gaussian distribution for  $\Phi_0 \ll E_F$ .

barrier height hence increase of tunneling current.

Another noticeable feature in Fig. 3 is that the logarithm of the scaled average current  $\log(J_{av}/J_0)$  can be fitted well with the functional form  $f(\sigma) = \alpha\sigma^2$ , where  $\alpha$  is a fitting parameter. This clearly shows that  $J_{av}$  follows Gaussian behaviour  $J_{av} = J_0 \exp(\alpha\sigma^2)$ . The fitting parameter  $\alpha$  in general depends on  $\Phi_0, \mathcal{E}$  and  $E_F$ . The dependence of  $\alpha$  with  $\Phi_0$  is nearly linear as shown in the inset of Fig. 3.

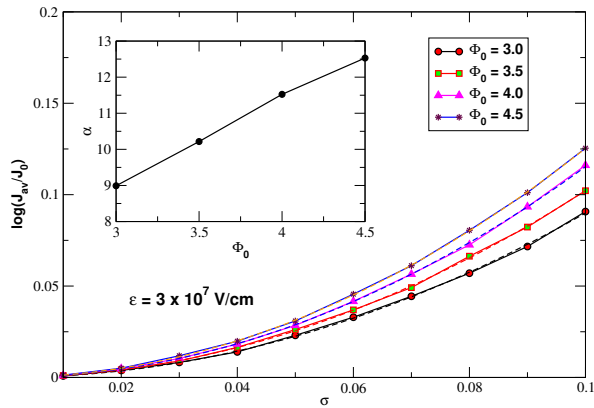


FIG. 3: (Color online) Logarithm of the scaled average current,  $J_{av}/J_0$ , as a function of the width,  $\sigma$ , of the work function distribution for various average work function,  $\Phi_0 \ll E_F$ . Solid lines with symbols are the numerical data and the dashed lines represents fitting function  $f(\sigma) = \alpha\sigma^2$ . Inset : variation of the fitting parameter  $\alpha$  with  $\Phi_0$ . The strength of the electric field,  $\mathcal{E} = 3 \times 10^7$  V/cm, and Fermi energy  $E_F = 10.0$  eV for all the cases.

In Fig. 4 we show the behaviour of  $\log(J_{av}/J_0)$  for various field strength  $\mathcal{E}$  as well as  $\Phi_0$ . For  $\mathcal{E} = 10^7$  V/cm

the increase of  $J_{av}$  is more than  $e$  times over the bulk value  $J_0$  for  $\sigma = 0.1$ . This can be explained by the fact that the tunneling current  $J \propto \frac{\mathcal{E}^2}{\Phi} \exp(-\zeta\Phi^{3/2}/\mathcal{E})$ . With increasing field strength the tunneling current dramatically increases mainly due to its  $\exp(-1/\mathcal{E})$  dependence. Averaging over work function distribution increases tunneling current as explained earlier. However this effect becomes sub-dominant for larger field strengths as the tunneling current increases over several orders of magnitude for just one order of magnitude increase of  $\mathcal{E}$ . The behaviour is similar for all the four choices of  $\Phi_0$ . In the inset of each plot in Fig. 4 we have shown the dependence of fitting parameter  $\alpha$  with the field strength  $\mathcal{E}$ . As can be clearly seen  $\alpha$  very strongly depends on  $\mathcal{E}$ .

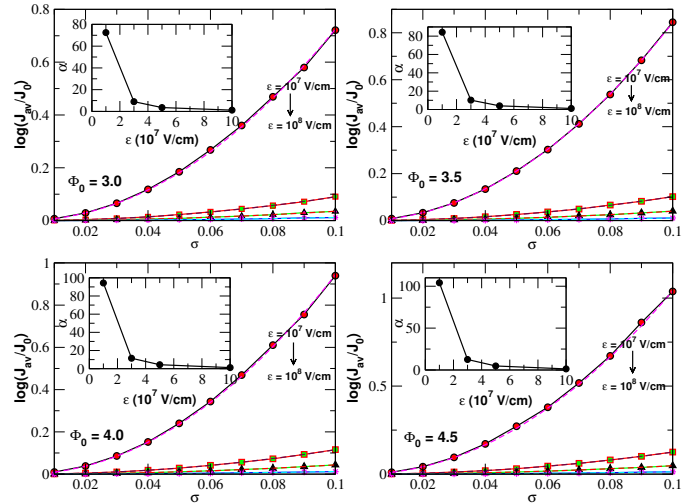


FIG. 4: (Color online) Panel plot : Logarithm of scaled average current,  $J_{av}/J_0$ , as a function of the width,  $\sigma$  of the work function distribution for various field strength,  $\mathcal{E}$ . Solid lines with symbols are numerical data and the dashed lines represent fitting function  $f(\sigma) = \alpha\sigma^2$ . Inset of each plot shows variation of  $\alpha$  with field strength,  $\mathcal{E}$ . The value of  $\Phi_0$  is indicated in each plot and  $E_F = 10.0$  eV for all the plots.

## 2. Case with $\Phi \gg E_F$

Next we consider the case with  $E_F = 0.05$  eV and  $\Phi_0 = 3.0, 3.5, 4.0$  and  $4.5$  eV. This will correspond to systems with low density as  $E_F \propto n^{2/3}$ . In this case the tunneling current does not depend on the prefactor  $\frac{e^3 \mathcal{E}^2}{16\pi^2 \hbar \Phi} \frac{[1-u(y_0)]}{t^2(y_0)}$  but still depends on the standard exponential factor  $\exp(-\zeta\Phi^{3/2}/\mathcal{E})$ . In Fig. 5 we show  $J_{av}$  as a function of  $N$ , the number of random variables for averaging over work function distribution for  $\Phi_0 = 3.0, 3.5, 4.0$  and  $4.5$  eV. As can be clearly seen  $J_{av}$  is atleast one order of magnitude smaller than the case with  $\Phi \ll E_F$ . This is mainly due to the fact that the prefactor  $\frac{me}{2\pi^2 \hbar^3} E_F^2$  for tunneling current  $J$  in this case is much smaller than the

prefactor  $\frac{e^3 \mathcal{E}^2}{16\pi^2 \hbar \Phi} \frac{[1-u(y_0)]}{t^2(y_0)}$  corresponding to the case with  $\Phi_0 \ll E_F$ . As in the earlier case  $J_{av}$  shows significant fluctuation for  $N < 10^4$ . We choose  $N = 10^5$  for various  $\Phi_0$  and  $\mathcal{E}$ .

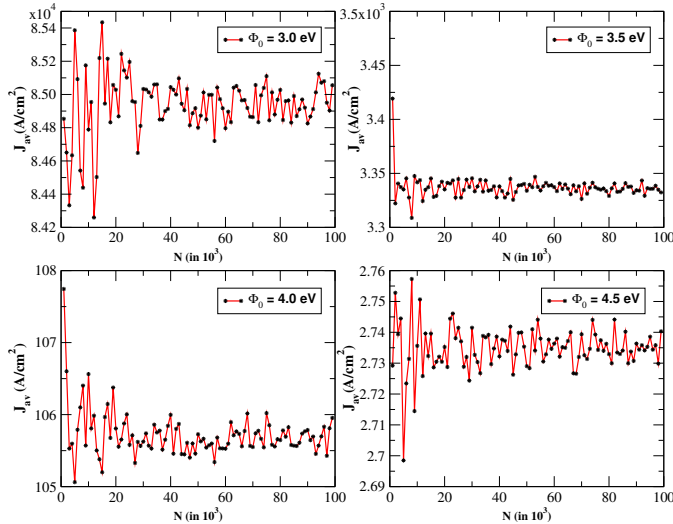


FIG. 5: (Color online) Average current,  $J_{av}$ , as a function of number of random variables,  $N$ , chosen from Gaussian distribution for  $\Phi_0 \gg E_F$ .

In Fig. 6 we show  $\log(J_{av}/J_0)$  as a function of the width,  $\sigma$ , of the Gaussian work function distribution for a given applied electric field strength  $\mathcal{E} = 3 \times 10^7$  V/cm. As in the case with  $\Phi_0 \ll E_F$ ,  $J_{av}$  monotonically increases with  $\sigma$ . But the increase is slower than the case with  $\Phi_0 \ll E_F$ . This is mainly because of the absence of  $\Phi$  dependent prefactor in the expression for  $J$ . Most interestingly, as in the earlier case with  $\Phi_0 \ll E_F$ ,  $\log(J_{av}/J_0)$  can be well fitted with  $f(\sigma) = \alpha\sigma^2$ . The fitting parameter  $\alpha$  linearly depends on  $\Phi_0$ .

In Fig. 7 we show the dependence of  $\log(J_{av}/J_0)$  with  $\sigma$  for various field strength  $\mathcal{E}$  and  $\Phi_0$ . As in the case with  $\Phi_0 \ll E_F$ , effect of work function distribution is strongest for the weakest field  $\mathcal{E} = 10^7$  V/cm. The tunneling current for  $\mathcal{E} = 10^7$  V/cm is very small ( $10^{-10}$  A/cm<sup>2</sup>) and very small change (lowering) of potential barrier can have much larger effect. With increasing field strength by one order of magnitude changes the tunneling current by several orders of magnitude which largely cancels the effect of work function distribution. However for each case  $\log(J_{av}/J_0)$  can be fitted well with  $f(\sigma) = \alpha\sigma^2$ . The fitting parameter  $\alpha$  strongly depends on  $\mathcal{E}$  as shown in the inset of each plot.

### B. Log-normal work function distribution

Next we consider log-normal distribution for the work function. In Fig. 8 we show the histogram plot of the work function, sampled over log-normal distribution for four choice of median work function  $M \equiv e^\mu =$

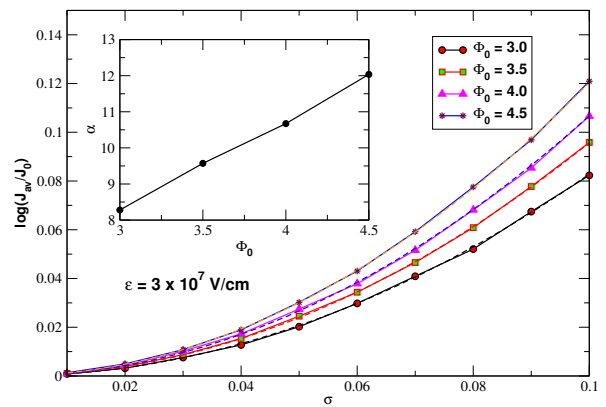


FIG. 6: (Color online) Logarithm of scaled average current,  $J_{av}/J_0$ , as a function of the width,  $\sigma$ , of the Gaussian work function distribution for various average work function,  $\Phi_0 \gg E_F$ . Solid lines with symbols are numerical data and dashed lines represents fitting function  $f(\sigma) = \alpha\sigma^2$ . Inset : variation of the fitting parameter  $\alpha$  with  $\Phi_0$ . The strength of the electric field  $\epsilon = 3 \times 10^7$  V/cm and  $E_F = 0.05$  eV.

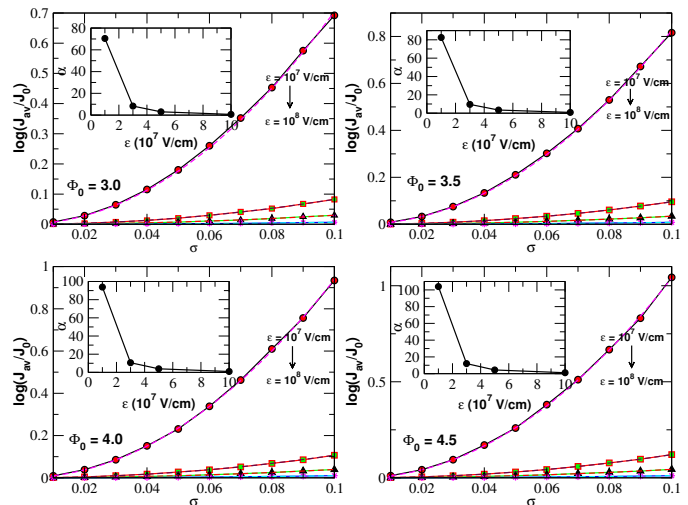


FIG. 7: (Color online) Panel plot : Logarithm of the scaled average current,  $J_{av}/J_0$ , as a function of the width,  $\sigma$  of the Gaussian work function distribution for various electric field strength,  $\mathcal{E}$ . Solid lines with symbols are numerical data and the dashed lines are fitting function  $f(\sigma) = \alpha\sigma^2$ . Inset of each plot shows the variation of  $\alpha$  with field strength,  $\mathcal{E}$ . The value of  $\Phi_0 \gg E_F$  is indicated in each plot and  $E_F = 0.05$  eV for all the plots.

3.0, 3.5, 4.0 and 4.5 eV with  $\sigma = 0.05$ . From this plot we can see that our choice of random variables for  $\Phi$  are well sampled over the log-normal distribution.

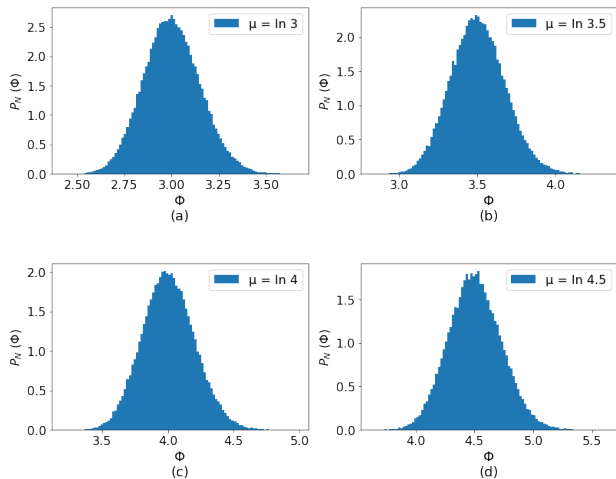


FIG. 8: (Color online) Histogram plot of work function,  $\Phi$ , sampled over log normal distribution for various  $\mu$  (see text). We have chosen  $\sigma = 0.05$  for all the figures.

### 1. Case with $\Phi \ll E_F$

First we consider the familiar case with  $\Phi \ll E_F$ . We choose  $E_F = 10$  eV and  $\mu = \ln 3.0, \ln 3.5, \ln 4.0$  and  $\ln 4.5$ . This will correspond to median value  $M = 3.0, 3.5, 4.0$  and  $4.5$  eV. In Fig. 9 we show  $J_{av}$  as a function of number of random variables for  $\Phi$ , chosen from log-normal distribution. The current density is several orders of magnitude higher than the case of Gaussian distribution. Also the fluctuations are higher than the case of Gaussian distribution. As in the earlier cases, we choose  $N = 10^5$  to get good statistical measure.

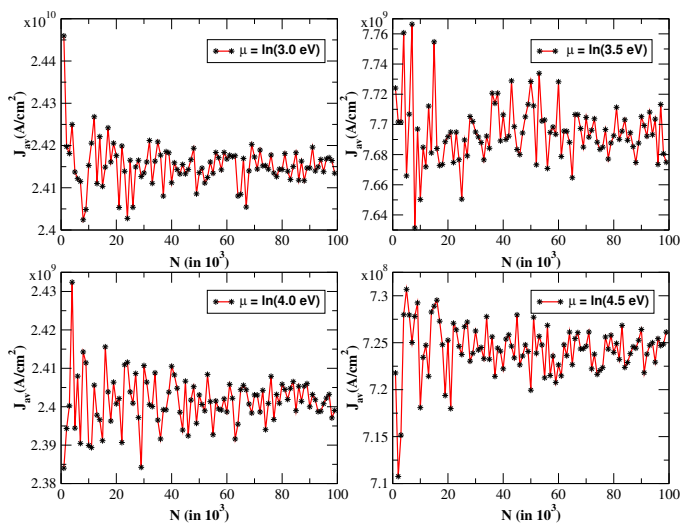


FIG. 9: (Color online) Average current,  $J_{av}$ , as a function of number of random variables,  $N$ , chosen from Log-normal distribution for  $\Phi \ll E_F$ .

In Fig. 10 we show  $\log(J_{av}/J_0)$  as a function of the width ( $\sigma$ ) of the log-normal work function distribution for  $M = 3.0, 3.5, 4.0$  and  $4.5$  eV and a given field strength  $\mathcal{E} = 3 \times 10^7$  V/cm, respectively. As in the case of Gaussian distribution,  $J_{av}$  increases monotonically as a function of the width of the distribution,  $\sigma$ . However the increase in this case is much stronger - more than 10 times  $J_0$  for  $\sigma = 0.1$ . This strong increase can be attributed to the skewness of distribution function. There is significantly higher probability of lowering of effective potential barrier than the Gaussian distribution with no skewness. As a result, the current density  $J \propto \exp(-\zeta\Phi^{3/2}/\mathcal{E})$  will show exponential increase with the width of the distribution. As shown in Fig. 10,  $\log(J_{av}/J_0)$  can be fitted well with the function  $g(\sigma) = \gamma\sigma^n$  with non-universal exponent  $n > 1$ . The fitting parameter  $\gamma$  increases linearly with the mean of the distribution.

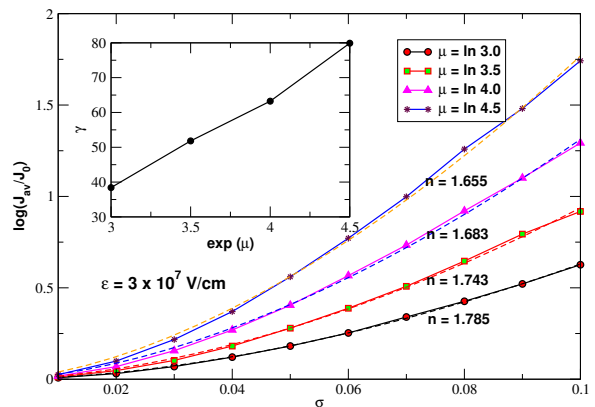


FIG. 10: (Color online) Logarithm of scaled average current,  $J_{av}/J_0$ , as a function of the width,  $\sigma$ , of the log-normal work function distribution for  $\Phi \ll E_F$ . Solid lines with symbols are numerical data and the dashed lines are fitting to  $g(\sigma) = \gamma\sigma^n$ , where  $n > 1$  is a non-universal exponent characterizing compressed exponential behaviour of  $J_{av}$ . Inset : variation of fitting parameter  $\gamma$  with the median of the distribution  $M = \exp(\mu)$ . The value of the exponents  $n$  for each case is shown on the figure and the value of the field strength  $\epsilon = 3 \times 10^7$  V/cm and  $E_F = 10$  eV.

In Fig. 11 we show  $\log(J_{av}/J_0)$  as a function of the width,  $\sigma$ , of the log-normal work function distribution for various field strength  $\mathcal{E}$  varying over one order of magnitude - from  $10^7$  V/cm to  $10^8$  V/cm. For the lowest field  $\mathcal{E} = 10^7$  V/cm,  $J_{av}$  increases by several orders of magnitude over  $J_0$ . This is mainly because of the fact that low field tunneling current is very small and the effect of averaging over work function distribution together with the skewness of the distribution increases the tunneling current drastically. Also the rise is near exponential as  $n \sim 1$ . With increasing  $\mathcal{E}$  the tunneling current increases and the effect of work function distribution gets largely suppressed. The fitting parameter  $\gamma$  strongly depends on the field strength  $\mathcal{E}$ .

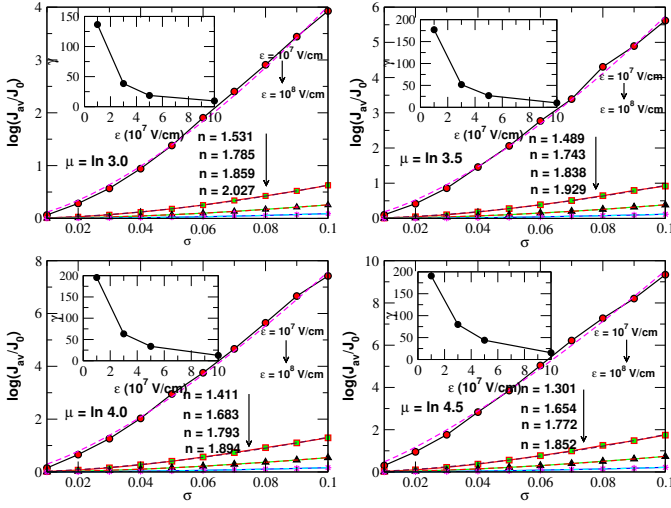


FIG. 11: (Color online) Panel plot : Logarithm of scaled average current,  $J_{av}/J_0$ , as a function of the width,  $\sigma$ , of the log-normal work function distribution for various applied field strength,  $\mathcal{E}$ .  $\mathcal{E}$  varies from  $10^7$  V/cm (top most curve) to  $10^8$  V/cm (bottom most curve) in each panel. Solid lines with symbols are numerical data and dashed lines represent fitting  $g(\sigma) = \gamma\sigma^n$ , where  $n > 1$  is non-universal exponent. Inset of each plot shows variation of  $\gamma$  with  $\mathcal{E}$  and the variation  $n$  is indicated in each plot.  $\mu$  is shown in each plot and  $E_F = 10.0$  eV for all the plots.

## 2. Case with $\Phi \gg E_F$

Finally we consider the case with  $E_F = 0.05$  eV and log-normal work function distribution. As in the other cases we first study the dependence of  $J_{av}$  on the number of random variables  $N$ . As shown in Fig. 12  $J_{av}$  shows strong fluctuations for  $N < 10^4$  and settles to a mean value for  $N > 6 \times 10^4$ . We choose  $N = 10^5$  for calculations. The magnitudes of currents are several orders of magnitude higher than the case of Gaussian distribution. However the currents are much smaller than the cases with  $E_F = 10.0$  eV and log-normal distribution.

In Fig. 13 we show  $\log(J_{av}/J_0)$  as a function of the width of the log-normal work function distribution for a given field strength  $\mathcal{E} = 3 \times 10^7$  V/cm for  $\mu = \ln 3.0, \ln 3.5, \ln 4.0$  and  $\ln 4.5$ , respectively. This choice of  $\mu$  corresponds to median value of the distribution  $M = 3.0, 3.5, 4.0$  and  $4.5$  eV, respectively. As in the earlier cases  $J_{av}$  monotonically increases with  $\sigma$ . As in the earlier cases  $\log(J_{av}/J_0)$  can be fitted well with  $g(\sigma) = \gamma\sigma^n$  with  $n > 1$ . The fitting parameter  $\gamma$  and the exponent  $n$  are nearly identical with the case with  $\Phi \ll E_F$ . With increasing  $M$ ,  $\log(J_{av}/J_0)$  increases and the exponent  $n$  decreases. This is because with increasing  $M$  ( $\Phi$ ) the tunneling current decreases and thereby enhances the work function distribution effect and near exponential increase in tunneling current with  $\sigma$ . The

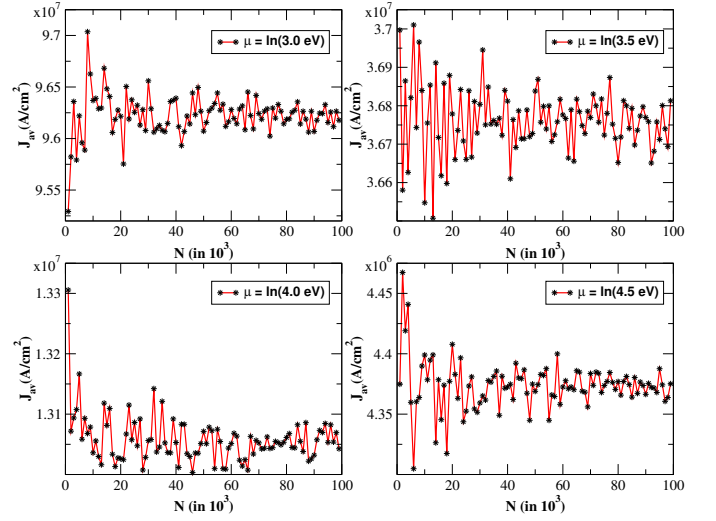


FIG. 12: (Color online) Average current ( $J_{av}$ ) as a function of number of random variables ( $N$ ) chosen from Log-normal distribution for  $\Phi \gg E_F$ .

fitting parameter  $\gamma$  behaves linearly with  $M = \exp(\mu)$

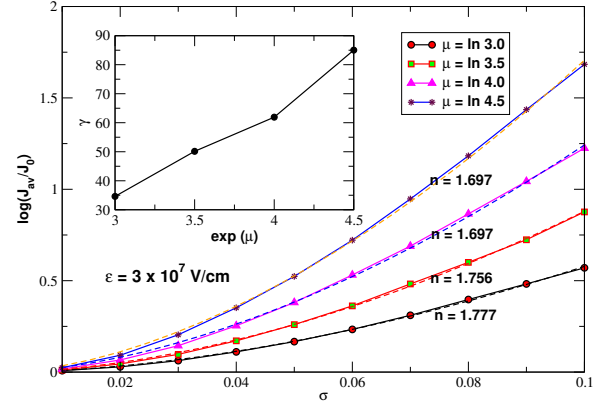


FIG. 13: (Color online) Logarithm of scaled average current,  $J_{av}/J_0$ , as a function of the width,  $\sigma$ , of the log-normal work function distribution for  $\Phi \gg E_F$ . Solid lines with symbols are numerical data and the dashed lines represent fitting  $g(\sigma) = \gamma\sigma^n$ , where  $n > 1$  is a non-universal exponent indicating compressed exponential behaviour of  $J_{av}$ . The value of  $n$  for each case is indicated in the figure. Inset : variation of  $\gamma$  with the median of the distribution  $\exp(\mu)$ . The applied field strength  $\epsilon = 3 \times 10^7$  V/cm and  $E_F = 0.05$  eV for all the cases.

In Fig. 14 we show  $\log(J_{av}/J_0)$  as a function of the width,  $\sigma$ , of the log-normal work function distribution for various field strength,  $\mathcal{E}$ , as well as the median of the distribution  $M = e^\mu$ . For the lowest field strength  $\mathcal{E} = 10^7$  V/cm the tunneling current,  $J_{av}$ , averaged over the work function distribution is several orders of magnitude larger than  $J_0$ , the tunneling current calculated with  $\Phi = M$ . As stated earlier this is due to the fact

that for  $\mathcal{E} = 10^7$  V/cm the tunneling current is very small and the skewness of the work function distribution effectively reduces the potential barrier significantly during the averaging process. With increasing field strength the tunneling current increases over several orders of magnitude and the effect of the work function distribution gets masked. With increasing  $M$  the tunneling current decreases and the work function distribution effect enhances. For each case  $\log(J_{av}/J_0)$  can be fitted well with  $g(\sigma) = \gamma\sigma^n$  with  $n > 1$ . The exponent,  $n$ , increases with the increasing field strength. For a given field strength,  $\mathcal{E}$ ,  $n$  decreases with increasing median value  $M$  of the work function distribution. In particular, for  $\mathcal{E} = 10^7$  V/cm  $n \sim 1$  giving rise to near exponential behaviour of the work function averaged tunneling current. The fitting parameter  $\gamma$  sharply decreases with increasing field strength.

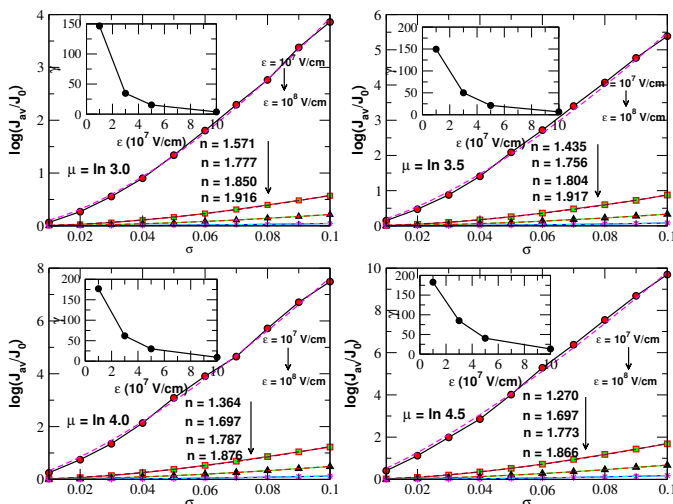


FIG. 14: (Color online) Panel plot : Logarithm of scaled average current  $J_{av}/J_0$ , as a function of the width,  $\sigma$ , of the log-normal work function distribution for various applied field strength,  $\mathcal{E}$ .  $\mathcal{E}$  varies from  $10^7$  V/cm (top most curve) to  $10^8$  V/cm (bottom most curve) in each plot. Solid lines with symbols are numerical data and the dashed lines represent the fitting function  $g(\sigma) = \gamma\sigma^n$ , where  $n > 1$  is non-universal exponent. The value of  $n$  for each curve is indicated in each plot. Inset of each plot shows variation of  $\gamma$  with the median of distribution  $\exp(\mu)$ . Value of  $\mu$  is explicitly shown in each plot and  $E_F = 0.05$  eV for each plot.

## V. CONCLUSIONS

In conclusion, we have considered the role of work function distribution on the tunneling current in field emission effect. We have calculated the tunneling current,  $J_{av}$ , averaged over work function distribution. We have considered both Gaussian as well as a log-normal work function distribution. For each case we have studied dependence of  $J_{av}$  on  $N$ , the number of random variables sampled over work function distribution.  $J_{av}$  shows significant fluctuations for  $N < 10^4$  but settles to an average value for  $N > 4 \times 10^4$ . We choose  $N = 10^5$  throughout the calculation. We first calculate  $J_0$ , the tunneling current calculated for  $\Phi = \Phi_0$  (Gaussian) or  $\mu = \ln M$  (log-normal), where  $\Phi_0$  or  $M$  (median of the distribution) corresponds to the *bulk value* of the work function. For each case we have studied the logarithm of the scaled current distribution  $\log(J_{av}/J_0)$  as a function of the width,  $\sigma$ , of the work function distribution for various  $\Phi_0$  (Gaussian) or  $M$  (log-normal) and the applied field strength  $\mathcal{E}$ . We have also considered systems with high density characterized by  $\Phi \ll E_F$  ( $E_F = 10$  eV) as well as systems with low density characterized by  $\Phi \gg E_F$  ( $E_F = 0.05$  eV). Both for Gaussian and log-normal distribution  $\log(J_{av}/J_0)$  increases monotonically with the increasing width,  $\sigma$ , of the work function distribution for a given field strength  $\mathcal{E}$ . This is due to the fact that averaging over work function distribution leads to exploration of the regions of lower potential height and hence increased tunneling current. The dimensionless quantity  $\log(J_{av}/J_0)$  can be fitted with  $f(\sigma) = \alpha\sigma^2$  (Gaussian) or with  $g(\sigma) = \gamma\sigma^n$  (log-normal). The fitting parameters  $\alpha$  and  $\gamma$  increases linearly with the bulk value of the work function i. e.  $\Phi_0$  (Gaussian) or  $M$  (log-normal). For log-normal distribution the non-universal exponent  $n > 1$  shows compressed exponential behaviour.

## Acknowledgements

We would like to thank Nei Lopes, Arghya Taraphder for many valuable discussions. One of us (N. P) would like to thank IIT, Kharagpur for local hospitality where part of the work was done. One of us (R. M) would like to thank Cetral Electronics Engineering Research Institute, Pilani for providing local hospitality and research support where part of the work was done.

<sup>1</sup> R. H. Fowler and L. Nordheim, Proc. Roy. Soc. London A, **119**, 173 (1928).  
<sup>2</sup> E. L. Murphy and R. H. Good, Phys. Rev., **102**, 1464 (1956).  
<sup>3</sup> T. C. Choy, A. H. Harker and A. M. Stoneham, J. Phys. Cond. Matt., **17**, 1505 (2005).  
<sup>4</sup> P. H. Cutler, J. He, J. Miller, N. M. Miskovsky, B. Weiss

and T. E. Sullivan, Progress in Surface Science, **42**,169185 (1993).  
<sup>5</sup> R. G. Forbes, K. L. Jensen, Ultramicroscopy, **89**, 1722 (2001).  
<sup>6</sup> C. J. Edgcombe, Phys. Rev. B, **72**, 045420 (2005).  
<sup>7</sup> K. L. Jensen and M. Cahay, Appl. Phys. Lett., **88**, 154105 (2006).



- <sup>8</sup> A. Fischer, M. S. Mousa, and R. G. Forbes, *J. Vac. Sci. Technol. B*, **31**, 032201 (2013).
- <sup>9</sup> R. G. Forbes, A. Fischer, and M. S. Mousa, *J. Vac. Sci. Technol. B*, **31**, 02B103 (2013).
- <sup>10</sup> A. Kyritsakis and J. P. Xanthakis, *Proc. R. Soc. A*, **471**, 20140811 (2015)
- <sup>11</sup> J. T. Holgate and M. Coppins, *Phys. Rev. Appl.*, **7**(4), 044019 (2017).
- <sup>12</sup> XLiana Gamez, Maxwell Terban, Simon Billinge and Maria Martinez-Inesta, **50**, 741 (2017).
- <sup>13</sup> Nei Lopes and A. V. Andrade-Neto, arXiv:1408.3663v3
- <sup>14</sup> Nei Lopes and A. V. Andrade-Neto, *Phys. Lett. A*, **384**, 126399 (2020).
- <sup>15</sup> D. Biswas and R. Ramachandran, *Phys. Plasmas* **24**, 073107 (2017).
- <sup>16</sup> A. Haug, *Theoretical Solid State Physics*, Volume 1, (Pergamon Press, Oxford, 1975.)
- <sup>17</sup> R. G. Forbes, *Appl. Phys. Lett.* **89**, 113122 (2006).
- <sup>18</sup> R. G. Forbes and J. H. B. Deane, *J. Vac. Sci. Technol. B*, **28**, C2A33 (2010).
- <sup>19</sup> W. W. Dolan, *Phys. Rev.* **91**, 510 (1953).
- <sup>20</sup> I. S. Gradshteyn and I. M. Ryzhik, *Tables of Integrals, Series and Products*. Academic, New York (1965).